Supplementary Information

Self-assembly of ultra-small micelles from amphiphilic lipopeptoids

K. H. Aaron Lau,[a,†] Valeria Castelletto,[b] Thomas Kendall,[c] Jan Sefcik,[d] Ian W. Hamley[b,†] Mehedi Reza,[e] Janne Ruokolainen[e]

[a] WestCHEM/Department of Pure & Applied Chemistry, University of Strathclyde, 99 George Street, Glasgow, G1 1RD, U.K.

[b] Department of Chemistry, University of Reading, Whiteknights, Reading RG6 6AD, U.K.

[c] EPSRC Doctoral Training Centre in Continuous Manufacturing and Crystallisation, Department of Chemical and Process Engineering, University of Strathclyde, 75 Montrose Street, Glasgow, G1 1XJ, U.K.

[d] Department of Chemical and Process Engineering, University of Strathclyde, 75 Montrose Street, Glasgow, G1 1XJ, U.K.

[d] Department of Applied Physics, Aalto University School of Science, P.O. Box 15100, FI-00076 Aalto, Finland

[†] Corresponding authors: Aaron.Lau@strath.ac.uk, I.W.Hamley@reading.ac.uk.

1. Material and Methods

1.1. Materials.

Palmitic acid (≥99%) and ACS reagent grade solvents (diethyl ether, dichloromethane, 2-propanol and methanol) were purchased from Sigma-Aldrich UK. 2-Phenylethylamine (99%), bromoacetic acid (BAA; 98+%), diisopropyl-carbodiimide (DIC; 99%), piperidine (99%), trifluoroacetic acid (TFA; 99%), N-Ethyldiisopropylamine (DIPEA; 99%) were Alfa-Aesar products purchased from VWR, UK. β-Alanine tert-Butyl Ester Hydrochloride (>98%) and N-(tert-Butoxycarbonyl)-1,2-diaminoethane (>97%) were purchased from TCI (Oxford, UK). Triisopropylsilane (Acros brand, 99%), sodium hydroxide (pellets/certified ACS), and HPLC grade acetonitrile were purchased from Fisher Scientific UK. Peptide synthesis grade N-methylpyrrolidone and dimethyl-formamide were purchased from Rathburn Chemicals (Walkerburn, Scotland). Rink amide-MBHA resin LL and O-(Benzotriazol-1-yl)-N,N,N',N'-tetramethyluronium hexafluorophosphate (HBTU) were purchased from Novabiochem/EMD Merck UK. All solvents and reagents were used as bought without further purification. Ultrapure (UP) water (resistivity =18.3 MΩ cm; total organic content of 5 ppb) was obtained from a Milli-Q Integral water purification system from EMD Merck UK.

1.2. Lipopeptoid Synthesis and Reverse-Phase High-Pressure Liquid Chromatography (RP-HPLC).

Submonomer peptoid synthesis was performed manually at room temperature following established protocol.[1, 2] Briefly, the resin was deprotected using 20% piperidine in NMP, left shaking for 20 min and repeated a second time. BAA at 20x excess of the resin loading was dissolved in DMF at between 1.5 M to 2.5 M, depending on size of the synthesis column and the amount of resin used. DIC was used at 18.5x excess. Bromoacetylation was allowed to proceed for 15 min. 20x excess amine submonomers were dissolved at 1M in NMP and the reaction was allowed to proceed for 60 min. For desalting the β-alanine tert-butyl ester HCl, 1.5x excess DIPEA relative to the amine was added in situ during the amine substitution reaction. The amine solution was captured after reaction and re-used 1-2 times. At the end of synthesizing the peptoid sequence, the N-terminus was capped with 4x excess of palmitic acid using HBTU coupling with 6x excess of DIPEA. Palmitic acid dissolved at a concentration of 0.5 M in DCM and HBTU was dissolved at 0.5 in DMF. These solutions were added to the resin before DIPEA was added. The reaction was allowed to proceed at 35°C for 2h, and then double coupled for a further 4h.

Resin cleavage and sidechain deprotection were accomplished together by treating the resin with 95% TFA (v/v), 2.5% UP water, and 2.5% TIPS for 15 min. The cleaved lipopeptoid was then removed by filtering and rinsing with TFA, and the solvent was removed using a rotary evaporator. The oily product was further dried under vacuum and purified by preparative gradient RP-HPLC (Dionex Ultimate 3000) using a 250x10 mm Phenomenex Jupiter C18 column. HPLC fractions containing the pure product were identified by ESI-LC-MS analysis (Agilent) and the ACN/water solutions were lyophilized. The purity of each final product was confirmed

by analytical RP-HPLC using a 250x4.6 mm diameter "Nucleosil" C18 column (Macherey-Nagel) and a gradient of 5-95% ACN run over 30 min.

1.3. Cryogenic Transmission Electron Microscopy (Cryo-TEM).

Experiments were carried out using a field emission cryo-electron microscope (JEOL JEM-3200FSC) operating at 300 kV. Samples were studied only at 1 wt.% peptide. P1, P2, P3 samples were dissolved in UP water. Sample was dissolved in water and the pH was fixed to 12.5 by titrating 0.98 M NaOH. Images were taken using bright-field mode and zero loss energy filtering (omega type) with a slit with 20 eV. Micrographs were recorded using a Gatan Ultrascan 4000 CCD camera. The specimen temperature was maintained at -187 °C during the imaging. Vitrified specimens were prepared using an automated FEI Vitrobot device using Quantifoil 3.5/1 holey carbon copper grids with 3.5 μm hole sizes. Grids were cleaned using a Gatan Solarus 9500 plasma cleaner just prior to use and then transferred into an environmental chamber of FEI Vitrobot at room temperature and 100% humidity. Thereafter, 3 μl of sample solution was applied on the grid, blotted once for 1 second and then vitrified in a 1/1 mixture of liquid ethane and propane at -180 °C. Grids with vitrified sample solutions were maintained in a liquid nitrogen atmosphere and then cryo-transferred into the microscope.

1.4. Small angle X-ray Scattering (SAXS).

Synchrotron SAXS experiments on solutions were performed on beamline BM29 at the ESRF (Grenoble, France) using a BioSAXS robot. P1, P2, P3 samples were dissolved in UP water. Sample N1 was dissolved in water and the pH was fixed to 12.5 by titrating 0.98 M NaOH. 1, 5 and 10 wt.% peptide solutions were loaded into the 96 well plate of an EMBL BioSAXS robot, and then injected via an automated sample exchanger into a quartz capillary (1.8 mm internal diameter) in the X-ray beam. The quartz capillary was enclosed in a vacuum chamber, in order to avoid parasitic scattering. After the sample was injected in the capillary and reached the X-ray beam, the flow was stopped during the SAXS data acquisition. BM29 operated with λ = 1.03 Å (12 keV). The images were captured using a PILATUS 1M detector. Data processing was performed using dedicated beamline software ISPYB (BM29). The data curves have been multiplied by an arbitrary constant in order to enable the visualisation of the data

1.5. SAXS Data Analysis.

The SAXS intensity from a scattering object without a particular orientation can be approximated by the following equation:[3]

$$I(q) \propto \left\langle F^2(q) S(q) \right\rangle \qquad (1)$$

where $F^2(q)$ is the scattering particle form factor and S(q) is the interparticle interference function. In this work we fitted the data within the approximation $S(q) \sim 1$.

The form factor was fitted according to a spherical core and shell model, characterized by a thickness of spherical shell (R_1), a radius of core (R_0), a total radius $R_0 + R_1 = R_{total}$ (D_{total}, = $2R_{total}$), a scattering length difference between shell and matrix (ξ), and a scattering density dif-

ference between core and matrix relative to the shell contrast (μ).[4] The data was fitted using SASfit software.[4]

1.6. Pyrene Fluorescence Assay.

The critical aggregation concentration (CAC) was determined via pyrene fluorescence measurements. The fluorescence of pyrene was excited at 335 nm at room temperature, and emission spectra were recorded from 360 to 460 nm using a 10.0 × 5.0 mm^2 quartz cell in a Varian Cary Eclipse spectrofluorimeter. Excitation and emission bandwidths of 2.5 nm were used throughout the experiments. The concentration of pyrene in water was 1.3 × 10^{-5} M. The same pyrene solution was used to dilute each peptide sample to avoid any dilution effect on pyrene fluorescence due to the addition of subsequent peptide amphiphile aliquots. Solutions were studied within the ranges (9×10^{-4} to 0.5) wt. % peptide dissolved in 1.3 × 10^{-5} M pyrene. The intensity of the peak centered around 373 nm is plotted in Figure 3.

1.7. Dynamic Light Scattering (DLS)

An ALV/LSE-5004 instrument was used to carry out dynamic light scattering experiments with a scattering angle θ = 90° and laser wavelength λ = 632.8 nm. The lipopeptoids were dissolved at a concentration of 0.3 wt.% in UP water. DLS is a technique that is commonly used to characterize nanoscale particles through measurements of the fluctuations in the scattered light intensity as a result of Brownian motion, which is dependent on the hydrodynamic radius of the particles. A normalised intensity autocorrelation function (ACF) for a monodisperse population of particles with a diffusion coefficient *D* decays exponentially as a function of the lag time, τ :

$$g_1(\tau) = e^{-\tau\Gamma} \qquad (1)$$

with a decay rate Γ:

$$\Gamma = Dq^2 \qquad (2)$$

where q is the scattering vector magnitude

$$q = \frac{2\pi n}{\lambda}\sin(\frac{\theta}{2}) \qquad (3)$$

n is the refractive index of water, θ is the scattering angle and λ is the laser light wavelength.

The initial decay rate Γ of the measured ACF is estimated using the cumulant analysis, the corresponded intensity weighted mean diffusion coefficient *D* is calculated from Eq. 2 and the Stokes-Einstein equation (Eq. 4) is used to calculate the mean hydrodynamic radius R_h:

$$R_h = \frac{(k_B T)}{6\pi\eta D} \qquad (4)$$

where k_B is Boltzmann constant, T is temperature and η is viscosity of water at the given temperature.

2. Supplementary data

2.1. Analytical HPLC of purified lipopeptoids

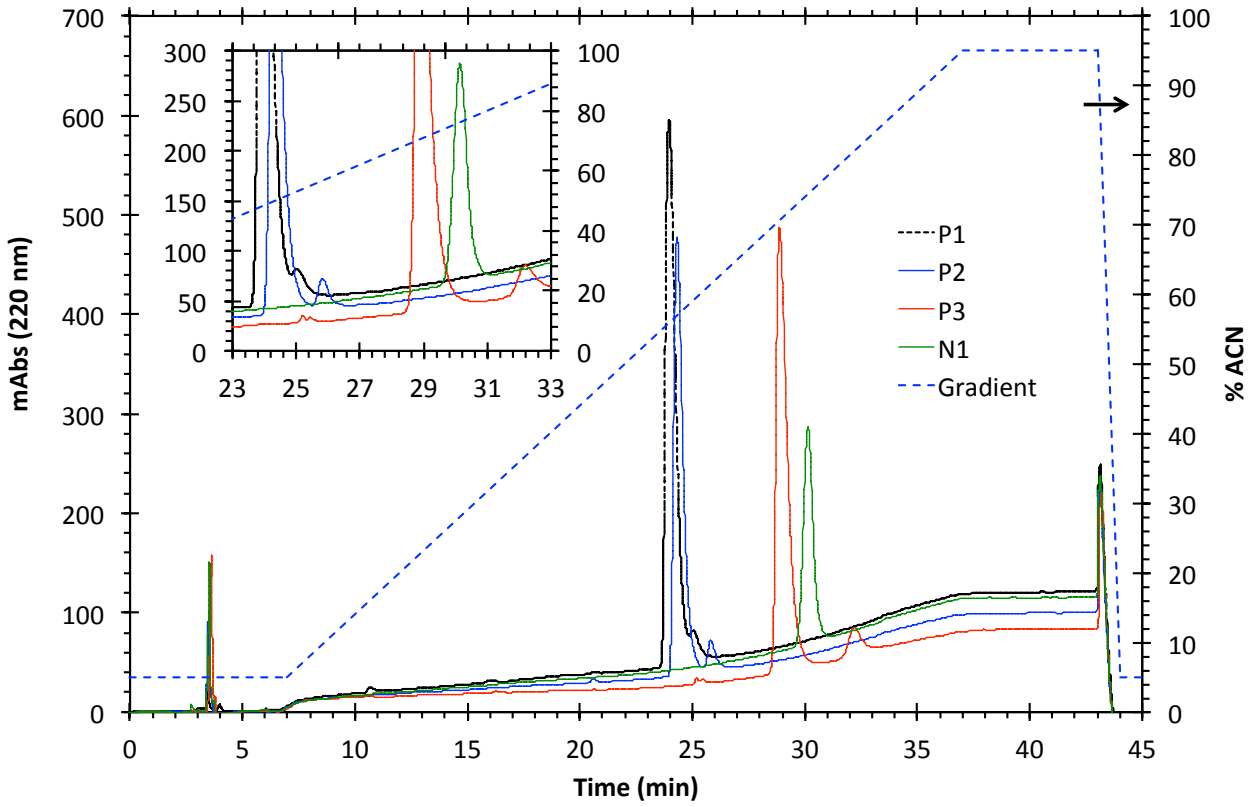

Figure S1. UV absorbance traces, measured at 220 nm, of the gradient analytical RP-HPLC elution of the pure lipopeptoid HPLC fractions collected during preparatory HPLC (see main text for sequence descriptions). A 5-95% ACN gradient over 30 min was used. A small peak always (re-)appeared between 1 to 3 min after the main elution peak for all the cationic P1/P2/P3 lipopeptoid species, even though the analytical samples were taken directly from fractions collected by the automated HPLC preparatory fraction collector (The P1 side peak at 25 min is convoluted with the main peak at 24 min but still clearly seen in the inset). It is likely that these small peaks correspond to the cationic P1/P2/P3 with fewer ionized sidechains (thus rendering the lipopeptoids more hydrophobic and resulting in later elution times). This interpretation is corroborated by the fact that no additional peaks appeared in the anionic N1 elution—the sidechains with carboxylic weak acids cannot ionize at the pH ~2 acidic conditions of the 0.1% TFA mobile phase used for measurements, and no other ionization state except the uncharged configuration is possible.

2.2. ESI-MS data verifying the masses of the synthesized lipopeptoids

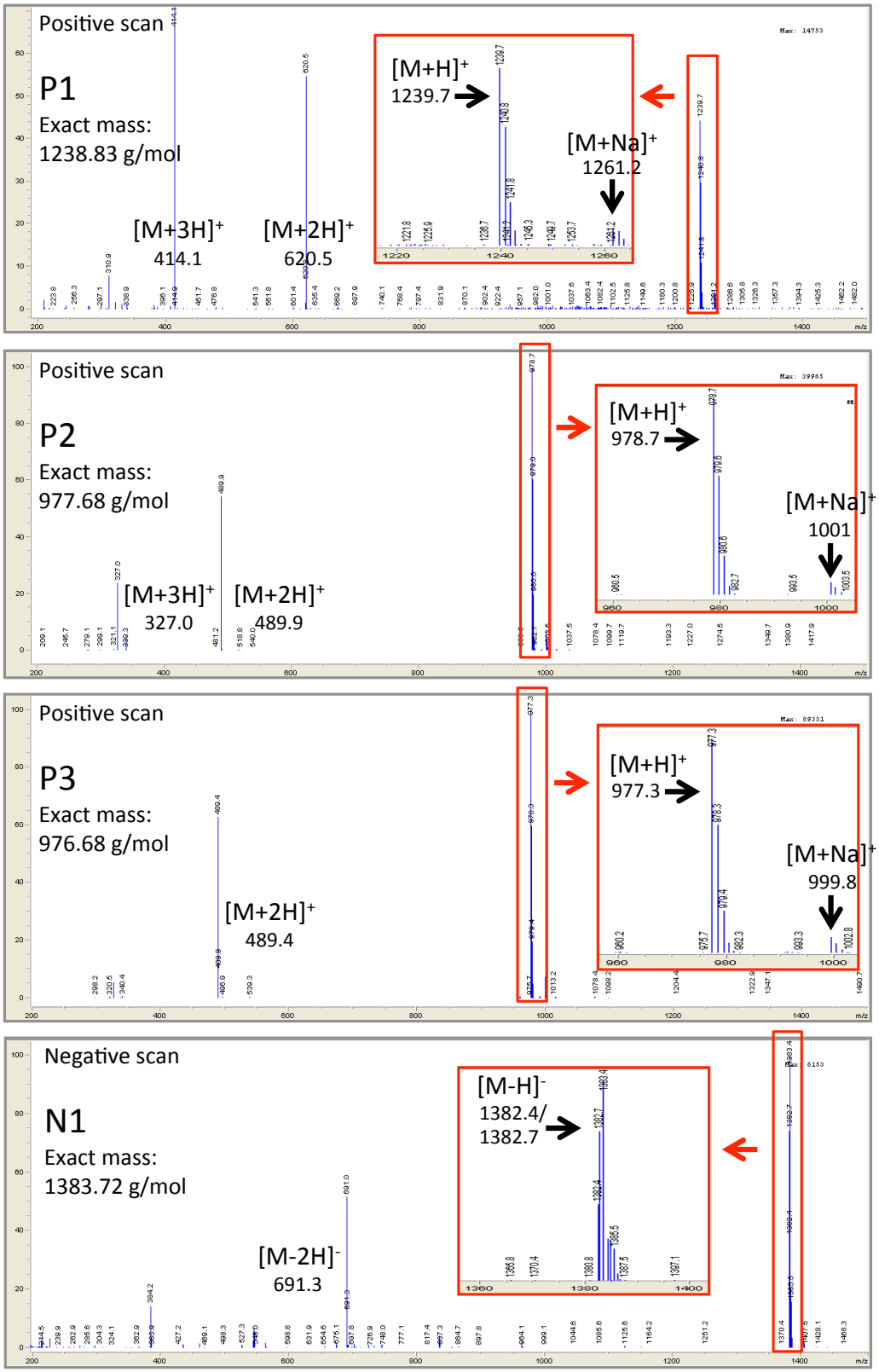

Figure S2. Mass spectrometry spectra (relative counts vs. mass/charge) of the purified fractions of the indicated lipopeptoids. P1, P2, P3 are cationic lipopeptoids, and positive fragments were analysed. N1 is an anionic lipopeptoid, and negative fragments were analysed. The actual counts corresponding to 100% are shown in the upper right corner of each panel (ranging from 8153 to 89331 counts).

2.3. Dissolution behaviour of lipopeptoids

The purified and lyophilized lipopeptoids were weighed and dissolved at known concentrations in ACN-water mixtures (between 20 to 60 mg of each purified species was obtained). 10 mg aliquots were distributed in separate 2 mL glass sample vials and lyophilised again. Dissolution tests consisted of pipetting known volumes of aqueous solutions into each vial and visually inspecting the samples to determine whether the dried lipopeptoids were dissolving or if turbidity appeared or aggregates remained. More sophisticated solubility/turbidity measurements (e.g. using UV-vis or DLS) could not be reliably performed due the small sample volumes available (from 100 to 300 ul for each sample). Where possible, the pH was measured using a "micro" glass probe that fitted through the opening of the vials. Otherwise, colour pH indicator paper was used. The recorded observations are listed below.

	Concentrations indicated below refer to the peptoid unless otherwise stated			
Solution composition	**P1**	**P2**	**P3**	**N1**
UP water (purified samples dried as TFA salts from HPLC fractions; lipopeptoids dissolved in pure water give acidic solutions)	7.3 mM Dissolves readily (pH 4.3) 0.2 mM Dissolves readily (pH 3.4)	102 mM Dissolves readily (< pH 2) 1 mM Dissolves readily (pH 2.3)	51 mM Mostly clear solution 2 mM in 5% ACN Dissolves readily (pH 2.5)	14.5 mM H2O Insoluble

Table S1. Dissolution behaviour of lipopeptoids in pure water.

pH	**2 mM N1**
4.8	insoluble (0.18 mM)
7.3	insoluble
9.0	insoluble
9.9	Insoluble
10.8	Insoluble
11.8	insoluble
12.2	insoluble
12.5	soluble
12.7	soluble

Table S2. Dissolution behaviour of the N1 lipopeptoids in aqueous solutions at various pH. Adding the lyophilized lipo-peptide in water resulted acidic solutions, since the peptoid was co-lyophilized with the 0.1 wt.% TFA used in HPLC solvents. NaOH was added to adjust the pH to higher values. The properties of the sidechains of Nglu should be analogous to its peptide counterpart Glu. Thus the pK_a of the carboxylate on the sidechain should be 4.2, and all the sidechains should have been completely ionized above pH 6~7. However, full dissolution of a solid piece of N1 material might require significant time. Moreover, the close proximity of neighbouring acid sidechains along the lipopeptoid means that a much higher driving force is likely required to ionize all the Nglu. The N1 solid was deemed to be insoluble if the dissolution was not immediate. These factors might have contributed to the highly basic conditions needed to dissolve N1.

2.4. Fluorescence spectra corresponding to the data shown in Figure 3 (critical aggregation concentration (CAC) assay).

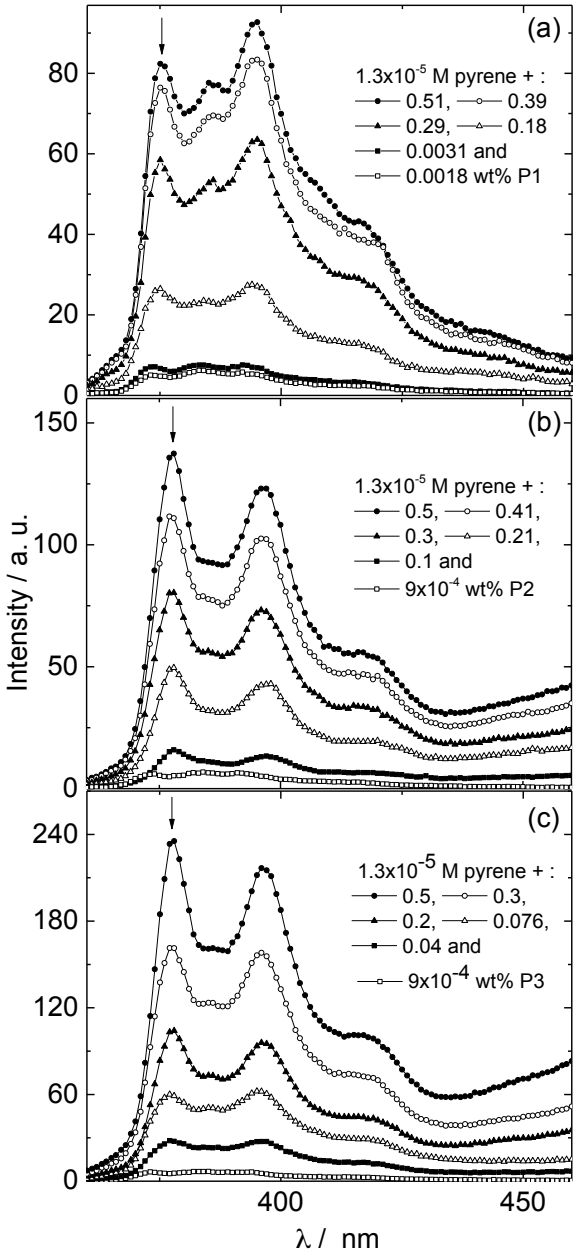

Figure S3. Representative pyrene fluorescence emission spectra for samples containing mixtures of pyrene and peptoids (a) P1, (b) P2 and (c) P3. The data series shown represent the range of concentrations used in the experiments; spectra taken below the CAC essentially overlap and are not shown for visual clarity. The fluorescence emission intensity plotted in Figure 3 corresponds to the maxima of the peak indicated with an arrow in (a-c) (centered around 373 nm).

2.5. DLS intensities and measurements after 11 weeks storage

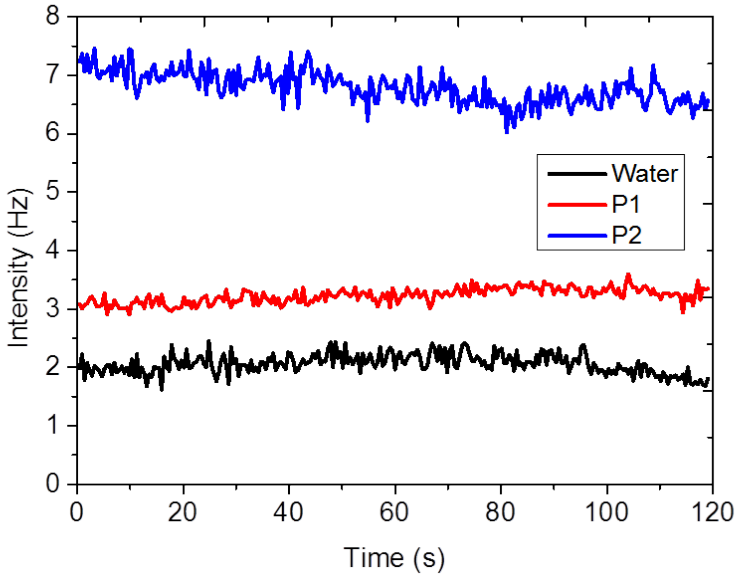

Figure S4. Scattered light intensities measured at 90° for P1 and P2 at 0.3 wt.% in UP water compared with measurement for the pure water control. The intensities measured for P1 and P2 samples are significantly higher than that measured for pure water.

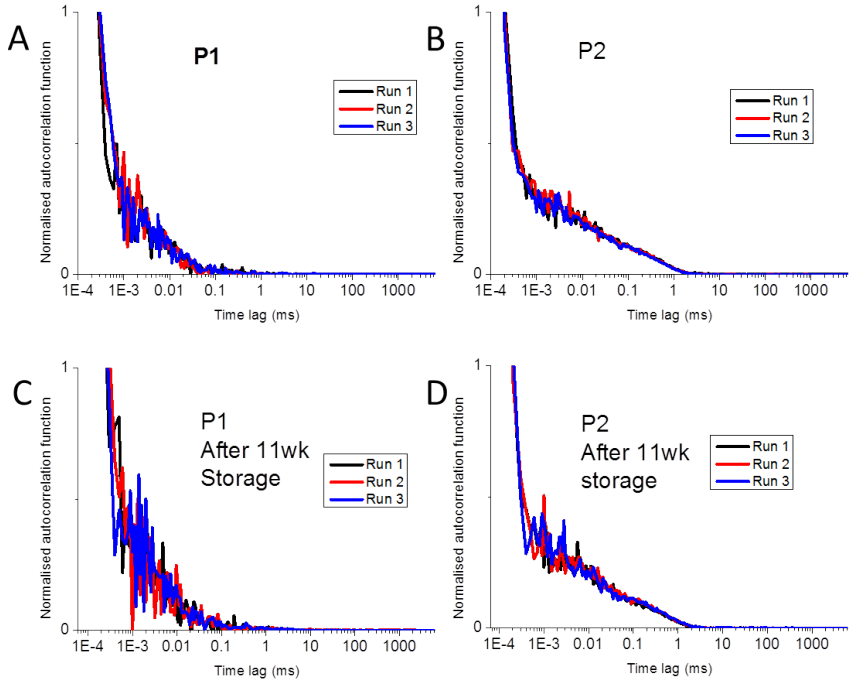

Figure S5. Normalised intensity autocorrelation functions (ACF) for P1 and P2 at 0.3 wt.% in UP water measured on the day the lipopeptoid solutions were prepared (A, B), and re-measured after 11 week storage at 4°C (C, D). Each solution sample was measured three times (runs 1 through 3 for each sample). Very similar trends were obtained before and after storage, although the ACF decay for P2 appears to extend slightly towards time lag ~3 ms after storage, indicating slight growth of the largest micelles/aggregates, even though the mean hydrodynamic radius Rh did not change significantly (see Table S3).

P1	10/06/16		26/08/16	
	Mean Radius (nm)	Intensity (Hz)	Mean Radius (nm)	Intensity (Hz)
Run 1	3	3.5	2	3.7
Run 2	2.3	2.9	3.25	3.2
Run 3	3	3.1	4.45	3.7
Average	2.77	3.17	3.23	3.53

P2	10/06/16		26/08/16	
	Mean Radius (nm)	Intensity (Hz)	Mean Radius (nm)	Intensity (Hz)
Run 1	25	6.9	20	7.4
Run 2	26	6.7	25	6.4
Run 3	30	7.4	30	7.3
Average	27	7.0	25	7.03

Table S3. Mean hydrodynamic radius R_h fitted for P1 and P2 (0.3 wt.% in water) before and after storage at 4°C for 11 weeks.

3. References

(1) Lau, K. H. A.; Sileika, T. S.; Park, S. H.; Sousa, A. M. L.; Burch, P.; Szleifer, I.; Messersmith, P. B., Molecular Design of Antifouling Polymer Brushes Using Sequence-Specific Peptoids. *Adv. Mater. Interf.* **2015,** *2*, 1400225.

(2) Zuckermann, R. N.; Kerr, J. M.; Kent, S. B. H.; Moos, W. H., Efficient method for the preparation of peptoids [oligo(N-substituted glycines)] by submonomer solid-phase synthesis. *J. Am. Chem. Soc.* **1992,** *114*, 10646-10647.

(3) Pedersen, J. S., Analysis of small-angle scattering data from colloids and polymer solutions: modeling and least-squares fitting. *Adv. Colloid Interface Sci.* **1997,** *70*, 171-210.

(4) Bressler, I.; Kohlbrecher, J.; Thunemann, A. F., SASfit: a tool for small-angle scattering data analysis using a library of analytical expressions. *J. Appl. Crystallogr.* **2015,** *48*, 1587-1598.